Nuclear Instruments and Methods in Physics Research B 270 (2012) 23–27

Contents lists available at SciVerse ScienceDirect

Nuclear Instruments and Methods in Physics Research B

journal homepage: www.elsevier.com/locate/nimb

Development of pulsed positron beam line with compact pulsing system

Masaki Maekawa *, Atsuo Kawasuso

Advanced Science Research Center, Japan Atomic Energy Agency, 1233 Watanuki, Takasaki, Gunma 370-1292, Japan

ARTICLE INFO

Article history:
Received 29 July 2011
Received in revised form 30 September 2011
Available online 20 October 2011

Keywords:
Slow positron
Pulsed positron beam
Positron annihilation lifetime spectroscopy
RF method

ABSTRACT

We have developed a pulsed slow positron beam with a pulse width of less than 200 ps and a period of 25 ns. The beam apparatus is composed of a Munich-type pre-buncher, a chopper and a buncher. Instead of the conventional RF cavity, a simple double-cylinder electrode is used for the buncher. The beam will be used for positron lifetime measurements. The time resolution of the whole system including lifetime measurement circuits is 250 ps, which is adequate for studying semiconductors and metals.

1. Introduction

Investigation of lattice defects in solids is important in the development of new functional materials. Positron annihilation spectroscopy is a powerful tool for detecting vacancy-type defects in materials: in particular, the presence and size of vacancy-type defects can be detected almost directly. The conventional positron lifetime measurement, which uses positrons directly emitted from radioisotopes, such as ^{22}Na, is suited to bulk studies [1–4]. However, for the study of subsurface layers and thin films, slow positron beams should be employed [5–7]. A continuous slow positron beam can be generated by moderating fast positrons emitted from the source. To perform the positron lifetime measurements, start trigger signals are needed. One established method is to use a pulsed positron beam such that positrons arrive at samples at regular intervals [8,9]. Several pulsed positron beams have been developed [10–12]. The required characteristics are (i) short pulse width (e.g., <200 ps) to avoid degradation of the time resolution, (ii) ample pulse period (e.g., >10 ns) to observe long-lived components, (iii) adequate signal-to-noise (S/N) ratio (e.g., >10^3) to analyze lifetime spectra precisely and (iv) high pulsing efficiency to avoid the loss of positrons. Most systems developed so far are based on the combination of a chopper and buncher [13–18]. We have developed a pulsed positron beam with a sufficiently short pulse width and a relatively low frequency. This system has compact electrodes and is equipped with a main buncher driven at 80 MHz. A pre-buncher and a chopper driven at 40 MHz enable beam pulsing without using an RF cavity or other advanced RF techniques.

2. Concept and design

The time of flight, T, of a charged particle from a gap to a target is given by

$$T = \frac{L}{\sqrt{\frac{m}{2e}(E_0 + V(t))}} \quad (1)$$

where L is the distance from the gap to the target, E_0 is the initial positron energy and $V(t)$ is the electric potential at the gap [19]. Therefore, if $V(t)$ changes with high frequency, bunching will occur in a continuous beam. It is important to shorten the pulse width of a beam as much as possible to make measurements with high time resolution. However, the pulse width tends to become broader than expected due to the finite energy spread (typically several electron volts for a slow positron beam). Reduction of the pulse width can be achieved by shortening the time of flight, and hence the size of the pulsing system should be reduced in order to provide a small value for L. The electron potential $V(t)$ generated by an RF wave is a periodic function. This means that $V(t)$ is divided into two parts: an 'effective phase' causing beam convergence and an 'ineffective phase' causing beam divergence. When the RF frequency is high, a beam with a shorter pulse can be formed. However, the pulse interval also becomes shorter and it becomes impossible to maintain a long enough interval for positron annihilation lifetime spectroscopy (PALS) measurements. For this reason, the frequency is kept as low as possible. By increasing the frequency, moreover, unexpected influences such as stray capacitance are enhanced, and this complicates the design and operation of the pulsing system [20,21]. If the direct-current (DC) positron beam is bunched directly, a background component will be generated since the beam entering during the ineffective phase will be spread out in time. To increase the S/N ratio, a beam chopper is used to avoid injecting the beam during

* Corresponding author.
E-mail address: maekawa.masaki@jaea.go.jp (M. Maekawa and A. Kawasuso).

0168-583X/$ - see front matter © 2011 Elsevier B.V. All rights reserved.
doi:10.1016/j.nimb.2011.10.001

the ineffective phase. The beam chopper is driven at several tens of megahertz, synchronized with the buncher frequency. The installation of a pre-buncher in front of the chopper is known to be an effective method of maintaining beam intensity. We, therefore, designed a three-stage bunching system: (i) a pre-buncher (40 MHz, $1/t^2$ wave), (ii) a reflection-type chopper (40 MHz, sine-wave) and (iii) a main buncher (80 MHz, sine-wave). Fig. 1 shows a schematic drawing of our pulsed positron beam apparatus. Positrons generated by a positron source (^{22}Na, 2.96 GBq) are thermalized by using a tungsten-mesh moderator (wire diameter 2 μm, 100 mesh/in.) [22]. The diameter of the moderator is 7 mm. Slow positrons emitted from the moderator are extracted by a grid electrode (2 eV) and transported by a magnetic guiding field (0.02 T). This DC beam is first bunched at the pre-buncher with a 40 MHz sawtooth t^{-2} waveform and converted into a pulse beam with a cycle of 25 ns. The pulse width is assumed to be several nanoseconds. The pre-buncher is composed of three cylindrical electrodes with two gaps of 5 mm and diameter of 20 mm. The RF wave is applied to only the center electrode. In this type of buncher, a beam will cross a gap at the entrance and the exit of the center electrode. To make efficient use of the modulation energy after crossing the two gaps, the length of the center electrode is adjusted so that a beam can pass in a half cycle of the RF fed into the buncher. After the buncher gaps, a long drift space is usually necessary to ensure the time convergence of the modulated beam. In our pre-buncher, it is possible to do without such a long drift space after the buncher because the buncher electrode itself can function as a drift space. The focal length is shortened using the high-amplitude RF wave. Thus, the long drift space for beam convergence becomes unnecessary, and the full length of the buncher system can be shortened. The length of the pre-buncher designed in this study is only 100 mm. After the pre-buncher, positrons that can become background beam components are cut with a reflection-type chopper which consists of three tungsten meshes (100 wires/in.). The gap between the meshes is 3 mm. As a chopping waveform, a simple 40 MHz sine wave with DC offset was applied to the center mesh. After the chopper, a double-cylinder main buncher is installed. A 80 MHz sine wave with a DC offset of 100 V relative to the chopper is used for the bunching RF wave. Although the structure of this buncher is the same as that of the pre-buncher, a sine wave is used here because it is difficult to prevent the distortion of a t^{-2} waveform. Nevertheless, since the incident beam is already bunched, further bunching can be carried out using a simple sine wave. In order to use the modulation voltage effectively, the length of the buncher electrode is chosen so that the time for a beam to pass between the two gaps is equal to a half-cycle of 80 MHz. The total length of the buncher is 130 mm and the drift space is 200 mm. Finally, the positron beam is electrostatically accelerated in the gap between the drift electrode and the sample stage. Fig. 2 shows simulated time structures after the pre-buncher, chopper and main buncher. The simulation was carried out by the solving 1-dimensional equation of motion numerically with a Monte-Carlo method. Fig. 2a shows the result of the calculation of the time structure of the pre-bunched beam at the exit of the pre-buncher. The DC beam is converted to a bunched beam with a width of 3 ns. Although the left-hand side of the peak is smooth, the right-hand side is discontinuous. This is probably due to a small disturbance of the t^{-2} waveform at the end of its period. As seen from Fig. 2b, the pulse width at the exit of the chopper does not change much but the background components are suppressed. When operating all pulsing devices, the time structure at the sample position is shown in Fig. 2c. The beam acceleration energy is 2.5 kV and a pulsed beam with a width of 200 ps and a high S/N ratio can be generated using our design.

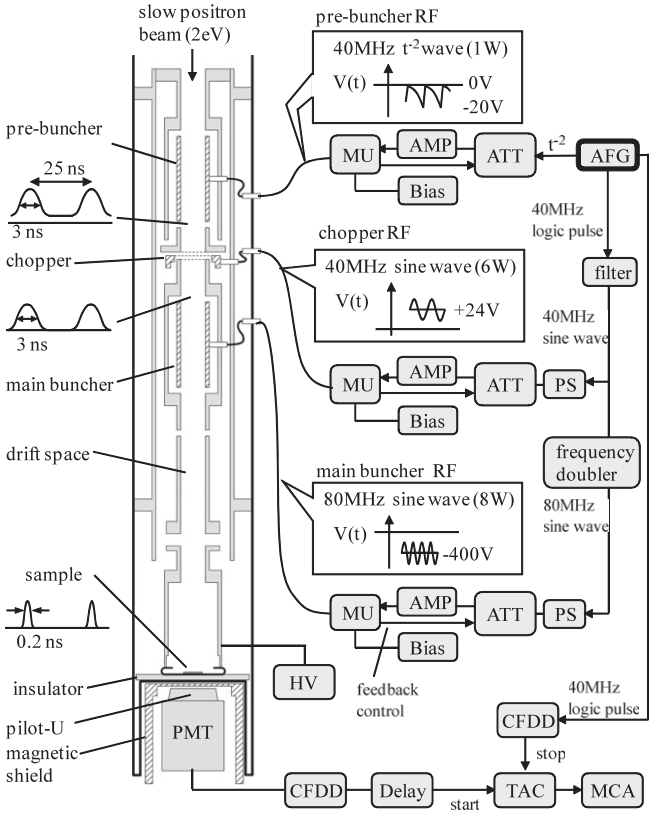

Fig. 1. Schematic drawing of out pulsing system and RF system. Abbreviations: AFG, arbitrary function generator; ATT, attenuator; AMP, power amplifier; MU, matching unit; PS, phase shifter; HV, high voltage; PMT, photomultiplier tube; CFDD, constant fraction differential discriminator; TAC, time-to-amplitude converter; MCA, multi-channel analyzer.

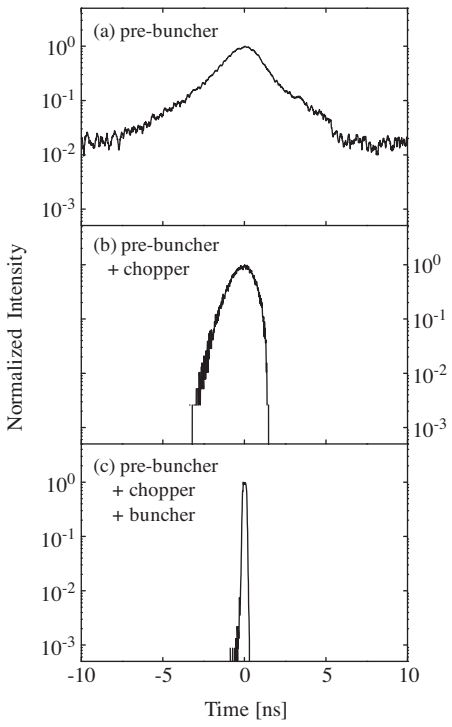

Fig. 2. Calculated time structures of pulsed beam. The calculation conditions are (a) only the pre-buncher, (b) pre-buncher and chopper and (c) the whole system.

3. Experimental procedure

As described in the Section 2, three types of DC-offset RF waves are required for this system. The t^{-2} waveform supplied to the pre-buncher is generated by an arbitrary function generator (AFG, Tektronix AWG510) and is amplified by an RF power amplifier (Thamway T142-432AA). A DC voltage is superimposed on the amplified waveform and fed to the pre-buncher as a waveform with $V = 0$ to -30 V. To suppress the distortion of the waveform, an impedance matching unit (MU) having the function of a DC block is installed between the pre-buncher electrode and the RF amplifier. This matching unit consists of capacitors and inductors. The voltage standing wave ratio (VSWR) is 1.28.

Although sine waves of 40 and 80 MHz are needed for the chopper and the main buncher, respectively, these must synchronize correctly with the pre-buncher. For minimum timing jitter, a sine wave of 40 MHz is generated from the 40 MHz rectangular pulse waveform output from the AFG. After adjustments of the signal timing using a phase shifter, this 40 MHz RF is split into two. One part is amplified with an RF amplifier (Thamway T142-4029A) and is fed into the chopper electrode through a matching unit. The distortion of the waveform becomes large because of the difficulty of giving a 50 Ω characteristic impedance to the chopper electrode due to the complex shape. However, this matching unit is designed as an LCR resonance circuit that operates at 40 MHz. Therefore, it is possible not only to produce a large amplitude in low power, but also to suppress the generation of unwanted harmonics. The VSWR of the RF system is 1.08. A 40 MHz sine wave of 6 W with a DC offset (+30 V) is provided to the chopper.

The other part of the 40 MHz sine wave is transformed to an 80 MHz sine wave using a frequency doubler to be the RF source of main buncher. A matching unit of the same type as the one described above is also installed. The VSWR of the RF system is 3.11. Thus an 80 MHz sine wave of 16 W with a DC offset (-100 V) is fed into the buncher.

A detector for the annihilation gamma rays is installed just behind the sample stage to record a counting rate. The detector is a Pilot-U scintillator with a photomultiplier tube (PMT, Hamamatsu H2431-50MOD). The time resolution of this PMT is easily degraded by an external magnetic field. Therefore, the whole detector was stored in a magnetic shield made of 45-permalloy (diameter of 80 mm and length of 400 mm). Using this shield, the guiding magnetic field of 0.02 T is decreased to 0.0005 T allowing normal operation of the PMT. The output signals are discriminated by the constant fraction difference discriminator (CFDD, ORTEC 583), and are used as start signals for the time to amplitude converter (TAC, ORTEC 556). The 40 MHz timing signal output from the AFG is input to the CFDD as a stop signal. Although the time-inverse spectrum is obtained, the deadtime of the TAC can be minimized because the conversion of the TAC is valid whenever the signal from the PMT is input.

4. Results and discussion

We first measured the time structures of the pulsed beam after the pre-buncher, chopper and main buncher using a high-speed microchannel plate (MCP) with an anode out (Hamamatsu F4655-13). Fig. 3a shows the time structure obtained after the pre-buncher. Convergence of the beam to a width of 3 ns was confirmed. The background level is high and S/N ratio is about 20 because of direct bunching of the DC beam. These values are in good agreement with the results of our calculations. A tail on the right-hand side of the peak appears, as expected from the calculations. Fig. 3b shows the time structure observed just behind the chopper. As expected, the background was greatly decreased and the S/N ratio increases to about 300:1, although the pulse width is unchanged. However, the background is not completely removed: possibly unthermalized high-energy positrons pass through the beam line to reach the MCP. This background is observed because the ratio of the dark current of the MCP itself to the background is about 1/3. Fig. 3c is the time structure of the pulsed beam at the sample position. The pulse width is 187 ps, which is in good agreement with the calculation. The S/N ratio is about 5000. Thus, the formation of a short-pulsed positron beam is confirmed. The flux of the pulsed beam is estimated to be approximately 1×10^4 positrons/s at the sample position. The efficiency of this pulsing system was about 1/6.

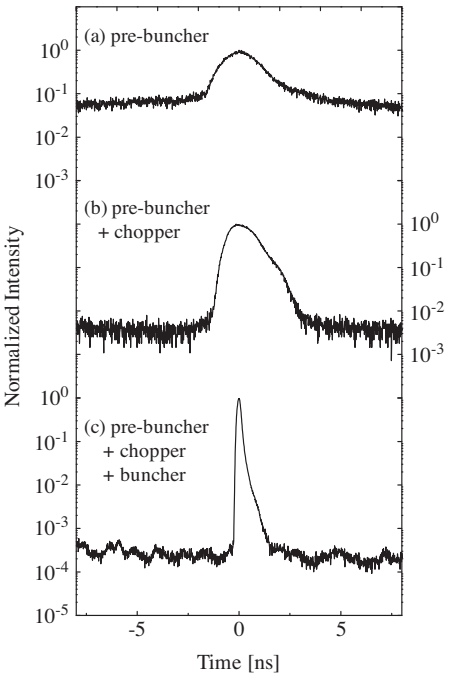

Fig. 3. Time structures of pulsed positrons detected by a micro-channel plate. The operation conditions are (a) only a pre-buncher, (b) pre-buncher and chopper and (c) the complete system.

Positron annihilation lifetime spectra for several reference samples were obtained. Table 1 shows the lifetime components analyzed by the PATFIT program [23] for each of the samples. The time resolution was approximately 280–300 ps. Fig. 4 shows the positron lifetime spectrum obtained for polyimide film. The incident positron energy was 7 keV. Open circles indicate the experimental results. The superimposed solid line shows the theoretical lifetime spectrum calculated by the PATFIT analysis. In the figure, theoretical lifetime spectra of each component and the residuals from the theoretical spectrum are also shown. From the PATFIT analysis, one single lifetime component ($\tau = 0.386$ ns) was obtained. This value is in good agreement with the reported value (0.382–0.386 ns) [24]. A satellite peak appears at around 7 ns from the peak. Since the distance from the sample surface to the acceleration gap is 100 mm and the expected time of the satellite peak is 6 ns, this satellite peak is attributed to positrons scattered from the sample surface.

Fig. 5 shows the positron lifetime spectrum of the *p*-type FZ-Si crystal. The incident energy was 19 keV. From the PATFIT analysis, two lifetime components were obtained: 0.22 and 1.01 ns with intensities of 97.2% and 2.7%, respectively. The shorter lifetime component can be attributed to the bulk silicon [25]. The longer one can be attributed to the influence of the natural oxidization layer which exists on the Si surface [26,27]. With increasing incident energy, the position of the satellite peak moves towards zero.

Table 1
Parameters obtained by fitting the lifetime spectra of the samples.

Sample material	Energy (keV)	τ^1 (ns)	τ^2 (ns)	τ^3 (ns)	I_1 (%)	I_2 (%)	I_3 (%)
Polyimide	7	0.386	–	–	100	–	–
FZ-Si (*p*-type)	19	0.220	1.010	–	97.2	2.7	–
Amorphous SiO_2	10	0.125(fixed)	0.555	1.549	21.7	18.4	59.9
PTFE	10	0.125(fixed)	0.380	2.999	13.1	60.8	26.0

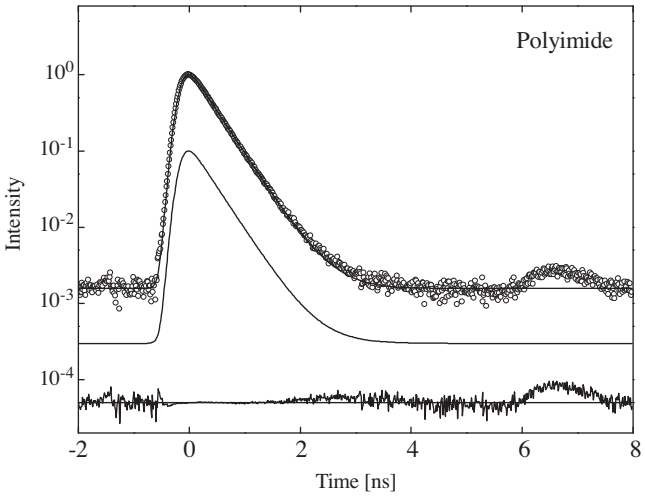

Fig. 4. The lifetime spectrum obtained for a polyimide film with an incident positron energy of 7 keV.

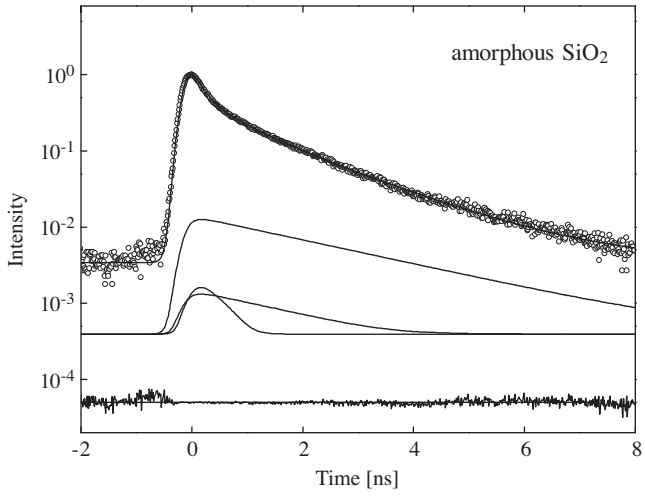

Fig. 6. The lifetime spectrum obtained for an amorphous SiO_2 substrate with an incident positron energy of 10 keV.

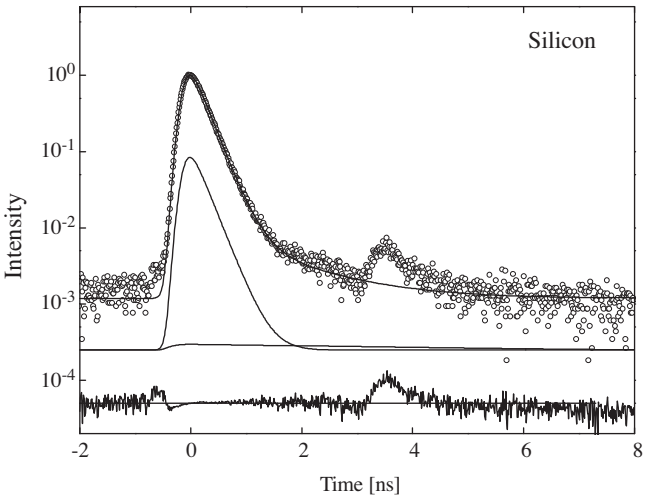

Fig. 5. The lifetime spectrum obtained for a *p*-type FZ-Si crystal with an incident positron energy of 19 keV.

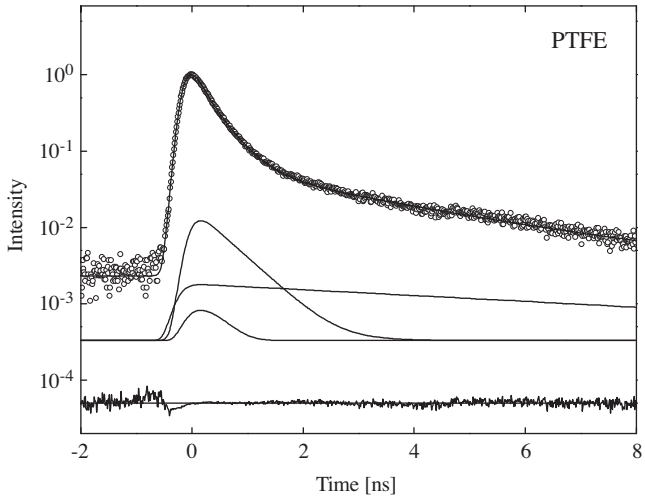

Fig. 7. The lifetime spectrum obtained for a PTFE sample with an incident positron energy of 10 keV.

Figs. 6 and 7 show the results of PALS measurements of an amorphous SiO_2 and a polytetrafluoroethylene (PTFE). It is known that these materials contain many large voids and positronium (Ps) will be generated. The shorter lifetime components (0.125 ns) of the annihilation of para-Ps and the longer lifetime components (several nanoseconds) from the pick-off annihilation of ortho-Ps are observed in addition to the lifetime components of free positron annihilation. From the PATFIT analysis, when the lifetime component of para-Ps is fixed to the 0.125 ns, two more lifetime components were obtained for these two specimens. The observed values are almost equivalent to the reported values [26,28].

Thus, it was confirmed that the PALS measurements including short lifetime components could be carried out with sufficient accuracy by this system. With the composition described above, the length of the whole buncher system was about 450 mm including an acceleration electrode. This is much more compact than existing pulsing equipment. Taking advantage of this size, the buncher system was made into a monolithic cartridge. Therefore, it is expected that the system can be easily installed in an existing beam line with a DC slow positron beam.

5. Summary

A slow positron pulsing system which can produce short pulses of positrons with time resolutions sufficient for PALS experiments has been developed and tested. This system is composed of three

parts: (i) a pre-buncher (40 MHz, t^{-2} wave), (ii) a reflection-type chopper (40 MHz, sine wave) and (iii) a buncher (80 MHz, sine wave). A complicated RF system is not needed because of the low-frequency operation. For this reason, this buncher system is designed with compactness in mind because this has a relatively small influence on ΔE of an incident beam and has contributed to the improvement in time resolution. Moreover, because of this compactness, the buncher system can be structured as a monolithic cartridge, which allows flexibility of installation. Positron annihilation lifetime spectra obtained using the beam showed a time resolution of 260 ps and a peak-to-background ratio of 1000:1 in PALS measurements for silicon. These values are in good agreement with the values expected from simulations.

References

[1] P.J. Schultz, K.G. Lynn, Rev. Mod. Phys. 60 (1988) 701.
[2] M.J. Puska, R.M. Nieminen, Rev. Mod. Phys. 66 (1994) 814.
[3] R.N. West, Positron Annihilation, Proceedings of the 7th international conference on Positron Annihilatio, New Delhi (World Scientific, Singapore) (1985) 11.
[4] P. Hautojärvi, Positron in Solids, Topics in Current Physics No. 12, Springer, Berlin, 1979.
[5] R. Suzuki, Y. Kobayashi, T. Mikado, H. Ohgaki, M. Chiwaki, T. Yamazaki, T. Tomimasu, Jpn. J. Appl. Phys. 30 (1991) L532.
[6] M. Hirose, T. Nakajyo, M. Washio, Mater. Sci. Forum 255–257 (1997) 674.
[7] N. Ohshima, E. Hamada, T. Suzuki, I. Kanazawa, Y. Ito, Mater. Sci. Forum 255–257 (1997) 629.
[8] R.C. Mobley, Rev. Sci. Inst. 34 (1963) 256.
[9] J.A.P. Mills, Appl. Phys. 22 (1980) 273.
[10] K. Fallstrom, T. Laine, Appl. Surf. Sci. 149 (1999) 44.
[11] J.D. Baerdemaeker, C. Dauwe, Appl. Surf. Sci. 194 (2002) 52.
[12] C. He, E. Hamada, N. Djourelov, T. Suzuki, H. Kobayashi, K. Kondo, Y. Ito, Nucl. Instrum. Methods B 211 (2003) 571.
[13] P. Willutzki, J. Stormer, G. Kogel, P. Sperr, D.T. Britton, R. Steindl, W. Triftshauser, Meas. Sci. Technol. 5 (1994) 548.
[14] P. Willutzki, J. Stormer, G. Kogel, P. Sperr, D.T. Britton, R. Steindl, W. Triftshauser, Mater. Sci. Forum 175 (1995).
[15] P. Sperr, G. Kogel, Mater. Sci. Forum 255–257 (1997) 109.
[16] T. Nakajyo, M. Hirose, Appl. Surf. Sci. 149 (1999) 34.
[17] E. Hamada, N. Ohshima, T. Suzuki, H. Kobayashi, K. Kondo, I. Kanazawa, Y. Ito, Appl. Surf. Sci. 149 (1999) 40.
[18] E. Hamada, N. Ohshima, T. Suzuki, H. Kobayashi, K. Kondo, I. Kanazawa, Y. Ito, Rad. Phys. Chem. 58 (2000) 771.
[19] D. Schodlbauer, P. Sperr, G. Kogel, W. Triftshauser, Nucl. Instrum. Methods B 34 (1988) 258.
[20] P.W.P. Sperr, M.R. Maier, Mater. Sci. Forum 175–178 (1995) 993.
[21] C. He, E. Hamada, T. Suzuki, T. Kumaki, H. Kobayashi, K. Kondo, Y. Ito, Appl. Surf. Sci. 221 (2004) 444.
[22] F. Saitoh, Y. Nagashima, L. Wei, Y. Itoh, A. Goto, T. Hyodo, Appl. Surf. Sci. 194 (2002) 13.
[23] P. Kirkegaard, N. Pederson, M. Eldrup, PATFIT-88, Riso-M-2704 (1989).
[24] S. McGuire, D.J. Keeble, Appl. Phys. 39 (2006) 3388.
[25] R. Krause-Rehberg, H.S. Leipner, Positorn Annihilation in Semiconductors, Springer, Berlin, vol. 27, 1998.
[26] M. Hasegawa, M. Tabata, T. Miyamoto, Y. Nagashima, T. Hyodo, M. Fujinami, S. Yamaguchi, Mater. Sci. Forum 175–178 (1995) 269.
[27] M. Hasegawa, M. Saneyasu, M. Tabata, Z. Tang, Y. Nagai, T. Chiba, Y. Ito, Nucl. Instrum. Methods B 166–167 (2000) 431.
[28] J.H. Green, S.J. Tao, Brit. J. Appl. Phys. 18 (1995).